International Journal of Scientific Engineering and Applied Science (IJSEAS) - Volume-1, Issue-7,October 2015
ISSN: 2395-3470
www.ijseas.com

Investigation of Mechanical, Thermal and Morphological Behavior of Cloisites-93A Clay Reinforced Poly (trimethylene terephthalate) Nanocomposites

Raghwendra Prakash Dwivedi[1], Arun Kumar Gupta[2], Bhagyashree[1] Smita Mohanty[2], S. K. Nayak*[1, 2]

Central Institute Of Plastics Engineering and Technology (CIPET)[1], Laboratory for Advanced Research in Polymeric Materials (LARPM)[2], Bhubaneswar, Odisha-751024, India

Abstract

Poly (trimethylene terephthalate) (PTT) nanocomposites constituting of variable wt. % of cloisites-93A (C-93A) clays were prepared using melt extrusion followed by microinjection molding process. Mechanical results revealed an improvement in tensile, flexural, and impact properties of PTT with 3 wt. % C-93A clay contents. The thermal properties of the nanocomposites have been investigated using HDT, DSC, and TGA. The heat deflection temperature (HDT) of the nanocomposites versus virgin PTT increased by up to 37 °C. The HDT increased monotonically with increasing clay content. In addition, the morphological changes in nanocomposites were also monitored through scanning electron microscopy (SEM) and transmission electron microscopy (TEM). Upon microscopic inspection, it was evident that clay infusion was achieved near the surface of the PTT matrix.

Keywords: Nanocomposites, Cloisites-93A, HDT, TGA, DSC, TEM

1. Introduction

The PTT nanocomposites attracted much attention out of many kinds of engineering plastic been used to prepare polymer nanocomposites. Several attempts have already been made by various researchers to enhance the mechanical and thermal properties of PTT, by adding clay, CNT, nanofiber and other fillers. Several studies on mechanical, thermal behavior of the PTT/clay nanocomposites [1], the PTT/CNT nanocomposites [2], the PA/clay nanocomposites [3], the PTT/EPDM-g-MA/clay nanocomposites [4], have shown that incorporation of 1 wt. % of nanofillers results in 10% increase in the mechanical properties.

Poly (trimethylene terephthalate) (PTT) biopolymer is prepared by the melt condensation polymerization of 1, 3-propandiol (derived from corn sugar) with either terephthalic acid or dimethyl terephthalate, it is a new aromatic polyester which can be used industrially due to the lowering of production cost and the can be easily obtained commercially in last decade [5]. PTT is a semi-crystalline with outstanding elastic recovery, relatively low melt temperature and rapid crystallization ability. PTT possess the desired attributes of thermoplastics polyester, wherein properties such as dimensional stability, solvent and abrasion resistance are pre-requisite [6]. However, certain impediments such as low toughness, viscosity, poor optical properties and pronounced low temperature brittleness have restricted the optimum use of PTT, as engineering plastic in many applications [7].

The properties of nanoclay dispersed polymer composites depend on the basal spacing of the nanoclay. Cloisite 10A, 15A, 25A, 93A, and 30B are some of the commercially available organo-nanoclay explored as nanofillers in polymer composites. Higher basal spacing enhances the degree of exfoliation and the modifier associated with the nanoclay provides better bonding and increases the interfacial strength of the composites resulting in superior mechanical and thermal properties [8].

Cloisite-93A is a commercially available organoclay having basal spacings of 23.6 Å which is greater than that of Cloisite Na (11.7 Å) but lower than that of Cloisite 15A (31.5 Å). Very few studies have been reported on the

influence of Cloisite 93A on the properties of the polymers [9].

In the present study PTT/C-93A clay nanocomposites were prepared using melt extrusion followed by micro-injection molding. The mechanical properties, thermal behavior, and morphology of nanocomposites were investigated.

2. Experimental

2.1 Materials

Poly (trimethylene terephthalate) (PTT) of grade PTT-1002 with intrinsic viscosity (IV) of 1.02 dl/g, melt flow index (MFI) of 19.3g/10 min, and density of 1.3 g/cc was supplied by M/s Dupont, Mumbai, India. Cloisites-93A (C-93A) clay with density of 1.88 g/cc was obtained from Southern Clay Products, Inc. All other solvents and chemicals of AR grade were purchased from M/s Mohaptara scientific Odisha, India.

2.2 Methods

Preparation of clay (C-93A) reinforced PTT nanocomposites

Nanocomposite of PTT/C-93A at various composition (99.0/1, 97.0/3.0, 95.0/5.0 by weight) were prepared using melt extrusion followed by injection moulding (Microcompounder with injection jet, X-Plore, DSM-Netherlands), at a screw speed of 45 rpm and 245^{0}C for a duration of 8 min. Prior to preparation, the PTT pellets were pre-dried at 110^{0}C for 24 hours in a vacuum oven and clays were pre-dried at 70^{0}C for 2 hours.

3. Characterization of PTT/C-93A clay nanocomposites

3.1 Mechanical properties

Tensile properties were determined using universal testing machine (UTM), Lloyd instruments ltd, UK, as per ASTM-D 638. Tensile test was performed using sample dimension of (127 X 12.7 X3) mm, at a cross-head speed of 10 mm/min and gauge length of 50 mm, whereas flexural test was determined, at cross-head speed of 1.5 mm/min and span length of 50 mm. Izod impact strength was measured using impacto-meter 6545 (CEAST, Italy) as per ASTM-D 256 with sample dimension of (63.5 X 12.7 X 3) mm.

3.2 Thermal properties

Differential scanning calorimetry (DSC) measurement were performed by scanning the (DSC Q 20, TA Instrument, USA), sample from 0-300^{0}C at the heating rate of 10^{0}C/min under nitrogen atmosphere. The thermal stability was studied from TGA/DTG curves using (TGA Q 50, TA Instruments, USA). Samples of about 10 mg were heated from 0-600^{0}C at a heating rate of 20^{0}C/min in nitrogen atmosphere.

3.3 Heat deflection temperature (HDT)

An HV-2000A-C3, GoTech, (Taiwan) analyzer was used to measure the heat-deflection temperature (HDT) of the PTT, and clays loaded nanocomposite. The HDT measurements were carried out in tensile mode using rectangular specimens of dimension (65 X 12.7 X 3) mm with a load of 66 psi and heating rate of 2^{0}C/minute.

3.4 Morphological characterization:

3.4.1 Scanning electron microscopy (SEM)

The morphologies of PTT and PTT-C-93A clay nanocomposites were examined employing SEM (EVO MA 15, Carl zeiss SMT, Germany). The samples were Au/Pd sputtered (50 nm) and dried for 30 minute at 70 ^{0}C in vacuum prior to study.

3.4.1Transmission electron microscopy (TEM)

For TEM observation, the samples were stained with uranyl acetate and were subsequently at low temperature (-55^{0}C) using Leica ultracut cryo-microtome (Japan) equipped with diamond knife. The ultra thin sections (50 nm, prepared from 3 mm thick plates) were examined using a transmission electron microscope TEM (JEM 1400, JEOL, Japan) using an accelerating voltage of 80 Kv at 100 nm scale.

4. Results and Discussions

4.1. Mechanical properties

Tensile strength, tensile modulus, tensile strain, flexural strength, flexural modulus, and

notched impact strength of the PTT and PTT/C-93A clay nanocomposites are listed in Table 1. The tensile strength (MPa) and modulus (MPa) were found to be 51.39, 52.72, 59.54, &, 53.28 and 1266.87, 1294.36, 1391.19, & 1332.30 for PTT, PTT/1%C-93A, PTT/3%C-93A, and PTT/5%C-93A clay nanocomposites, respectively. The highest tensile strength and modulus for PTT/3%C-93A clay nanocomposites are obtained and about 15.85 % and 9.81 % is higher than that of virgin PTT matrix. Whereas, the tensile strain also increases when the clay loading gradually increases up to 3 wt. % and decreases when the content of clay is 5 wt. % .

Furthermore, the relationship between the flexural properties and the organoclay content shows a similar trend. The difference is that the addition of only 5 wt% the organoclay causes dramatic decreases in the flexural strength and modulus. For example, the flexural strength and moduls of the PTT nanocomposite containing 3 wt. % C-93A clays are 79.77 MPa & 2890.17 MPa, which is 6.98 % and 17.12 % higher than that of the virgin PTT matrix. The change of the flexural modulus is different from that of the two above-mentioned properties. The flexural moduli of all the nanocomposites increase when the organoclays loading gradually increases up to 3 wt%.

Moreover, the notched Izod impact strength for the three different composition of clay containing of nanocomposite remains basically unchanged or experiences a slight decrease when the content of the organoclay is above 3 wt%.

This increase in the mechanical properties of the PTT is thought to be dependent on the interactions between the PTT molecules and the layered organoclays, as well as on the rigidity of the clay layers themselves. Indeed, the rigidity of the clay layers is considerably greater than the PTT molecules and thus they do not deform or relax to the same extent [10]. This improvement in the mechanical properties of PTT was possible because organoclay layers could be dispersed and intercalated effectively within the polymer matrix [11]. This is consistent with the general observation that the introduction of an organoclay into a matrix polymer is found to increase its strength and modulus. Results suggest that greater stretching of the clay leads to the occurrence of debonding around the polymer–clay interfaces [12]. This indicates that hydrostatic elongation during the extrusion and injection molding operations resulted in the debonding of the polymer chain itself. Moreover, the occurrence of imperfect bonding leads to debonding at the interface, giving rise to a constant interfacial shear stress when strain is applied to the nanocomposites [13].

Table 1: Mechanical properties of PTT & PTT/C-93A clay nanocomposites

Sample (wt. %)	Tensile strength (MPa)	Tensile modulus (MPa)	Tensile strain (%)	Flexural strength (MPa)	Flexural modulus (MPa)	Notched impact strength (J/m)
Virgin PTT	**51.34**	**1266.87**	**2.81**	**74.56**	**2467.57**	**32.45**
PTT/1% C-93A	**52.72**	**1294.36**	**3.13**	**76.58**	**2483.65**	**37.91**

PTT/3% C-93A	**59.54**	**1391.19**	**3.97**	**79.77**	**2890.17**	**44.86**
PTT/5% C-93A	**53.28**	**1332.30**	**3.25**	**78.95**	**2580.43**	**46.54**

4.2 Thermal properties

4.2.1 Thermogravimetric analysis (TGA): Thermal stability of the nanocomposites

Fig. 1 & Fig. 2 show the TGA and DTG thermogram of the PTT, and mechanically optimized PTT/3% C-93A clay nanocomposites, respectively. Virgin PTT exhibits an initial degradation temperature (i.e 10 wt. % loss) (T_{id}) of 352.45 °C with final degradation temperature (i.e 100 wt. % loss) (T_{fd}) 459.39 °C. Whereas, mechanically optimized PTT/3% C-93A clay nanocomposites exhibits an initial degradation temperature of 366.76 °C and final degradation temperature 464.16 °C, respectively. At 10 wt. % loss, PTT/3% C-93A clay nanocomposite shows higher initial and final degradation temperature as compared to virgin PTT. Similarly at 50 wt. % losses (i.e. maximum degradation temperature) PTT nanocomposites shows enhancement in the initial and final degradation temperatures indicating higher thermal stability in the nanocomposites as compared with the virgin matrix due to stable morphology of the dispersed phase & presence of intercalated silicate layers that might have contributed in enhanced thermal stability of the PTT nanocomposites [10]. The values of the decomposition temperature of PTT and PTT/3% C-93A nanocomposites are listed in Table 2. It is obvious that, the thermal stability of PTT nanocomposites increases. The improvement of thermal stability of the nanocomposites can be attributed to the shielding effect of clay. Small molecules generated during the thermal decomposition process cannot permeate but have to bypass clay layers. Thus, the addition of the organoclays slows down the release rate of decomposed byproducts and enhances the thermal stability of the nanocomposites [12]. From Table 2, one can see that *T*id for the PTT nanocomposites increases with containing 3 wt. % C-93A clays. However, the change of *T*id for the PTT/C-93A nanocomposites is regular, which is caused by homogeneous dispersion of the organoclays. In addition, it can be found from Table 2 that the PTT/3% C-93A clay nanocomposites possess better thermal stability than the PTT matrix. These results can be ascribed to the strong interaction between the PTT matrix and C-93A clay and the better dispersion of C-93A clay in the PTT matrix [16].

Table 2: Thermal stability of PTT and PTT nanocomposites

Sample (wt. %)	Initial degradation temperature (°C)	Maximum degradation temperature (°C)	Final degradation temperature (°C)
Virgin PTT	352.45	426.19	459.39
PTT/3% C-93A	366.76	430.96	466.16

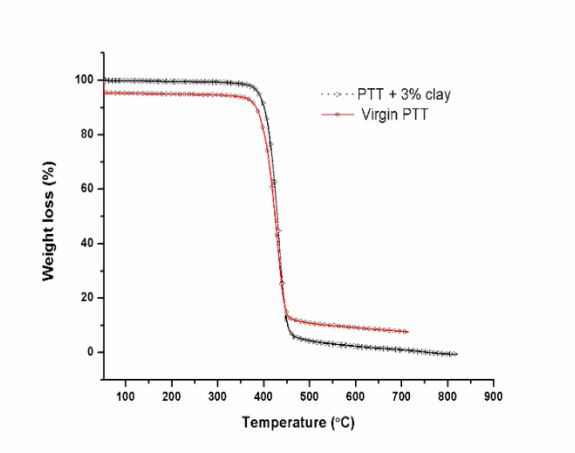

Figure 1: TGA thermaogram of PTT & PTT/C-93A clay nanocomposites

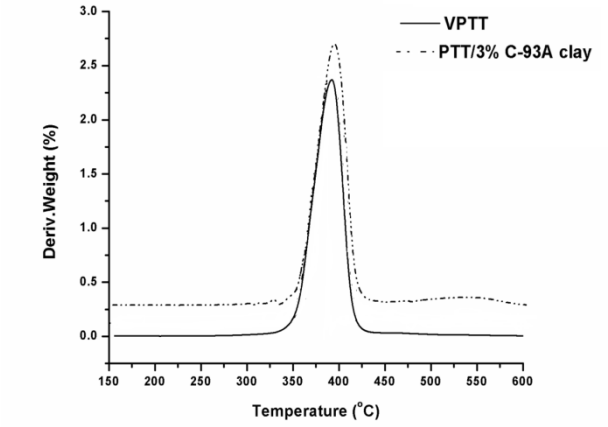

Figure 2: DTG thermaogram of PTT & PTT/C-93A clay nanocomposites

4.2.2 Differential scanning calorimeter (DSC)

Differential scanning calorimetry has been widely applied in the investigation of numerous phenomena occurring during the thermal heating of organoclays and polymer/clay nanocomposites, involving glass transition (Tg), melting, and crystallization [14]. Referring to clay nanocomposites, Differential Scanning Calorimetry (DSC) thermograms for melting and crystalline temperature of virgin PTT, and PTT/3% C-93A clay nanocomposites are enumerated in Figure 3 (a) and 3(b), respectively. Corresponding crystallization temperature (T_c), melting temperature (Tm), heat of fusion and degree of crystallinity values are also represented in Table3. From Figure 3 (a), virgin PTT exhibits T_m of 227.18 °C whereas PTT/3% C-93A clay nanocomposites show its corresponding T_m around 231.23 °C. In case of PTT nanocomposite there was a marginal increase of about 4 °C in T_m of PTT/3 % C-93A clay nanocomposites as compared with virgin PTT matrix. This indicates that the C-93A clay preferentially resides within the PTT matrix [15].

Furthermore, Figure 3 (b), shows the DSC cooling thermograms of PTT, PTT/3% C-93A clay nanocomposites. The crystallization peak temperature (T_c) of virgin PTT was observed around 174.7 °C which increased considerably to 187.6 °C with the incorporation of 3% C-93A clays. This confirms that the silicate layers acts as an efficient nucleating agent for the crystallization of PTT matrix [13].

Table 3: DSC results of PTT and PTT/C-93A clay nanocomposites

Sample (wt. %)	T_m (°C)	T_c (°C)	H_m (J/m)	X_c %
Virgin PTT	227.18	174.7	52.21	33.4
PTT/3% C-93A	231.23	187.6	56.46	34.7

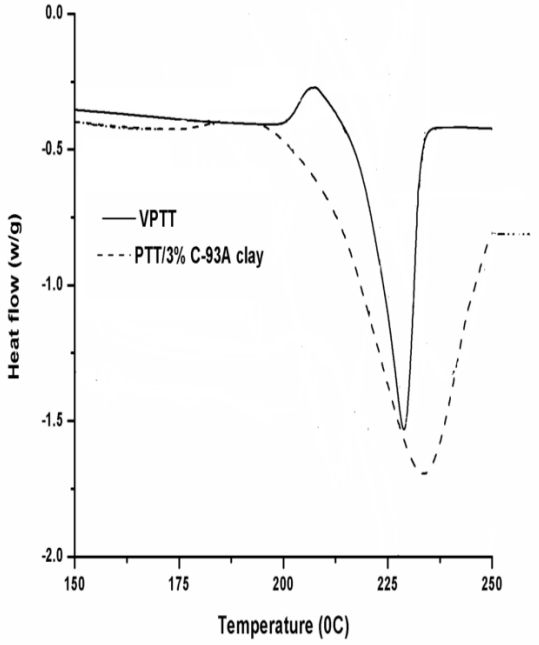

Figure 3 (a): DSC thermogram for melting temperature (T_m) of PTT & PTT/C-93A clay nanocomposites

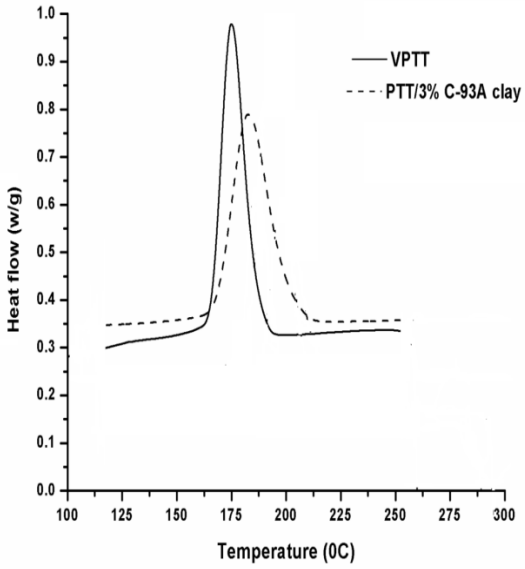

Figure 3 (b): DSC thermogram for crystalline temperature (T_c) of PTT & PTT/C-93A clay nanocomposites

4.2.3 Heat deflection temperature (HDT)

Heat deflection temperature (HDT) of a polymeric material is an index of heat resistance towards the applied load; the HDT of PTT and PTT/C-93A clay nanocomposites based on various proportions of wt% of C-93A clay contents are depicted in Figure 4. It can be seen that the HDT increases with increasing C-93A nanoclays, suggesting that clay layer have good effect on improving the thermal resistance of PTT. The HDT was 19.5 %, 38.26 % & 50.86 % increased of PTT/1%C-93A, PTT/3%C-93A, and PTT/5%C-93A clay nanocomposites as compared with virgin PTT matrix, respectively. These results suggest that improvement in HDT for PTT after nanocomposite preparation originates from the better mechanical stability, reinforcement by the dispersed nanoclays, and higher degree of crystallinity and intercalation of the nanocomposite as compared with virgin PTT matrix. According to results observed that the HDT rapidly increases with increasing C-93A clay content and reaches a maximum as C-93A clay content is 5 wt% because of the better clay-dispersion of C-93A in the PTT matrix promotes a higher HDT [12].

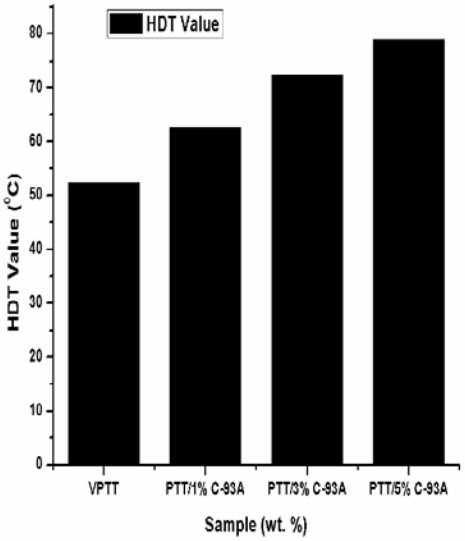

Figure 4: HDT value of PTT and PTT/C-93A clay nanocomposites

4.3 Morphology of the nanocomposites

4.3.1 Scanning electron microscopy (SEM)

The morphologies of the PTT and mechanically optimized PTT/3% C-93A clay nancomposites were examined by observing their fracture surfaces using SEM Figs. 5 (a) & 5(b). Figure 5 (a) indicates that the PTT surface is smooth and fine micrograph. Fig. 5(b) reveals that C-93A clay phases were formed within undrawn PTT matrix with content of 3 wt%. These PTT nanocomposites exhibited morphologies consisting of clay domains of about 50-60 nm in size, and fully dispersed in a continuous PTT phase [12]. The domain size of the dispersed clay phase and the formed voids are observed to decrease slightly with increasing clay. These results appear to be the consequence of excess stretching of the nanocomposites when the extrudates pass through the micro-injection molding [13].

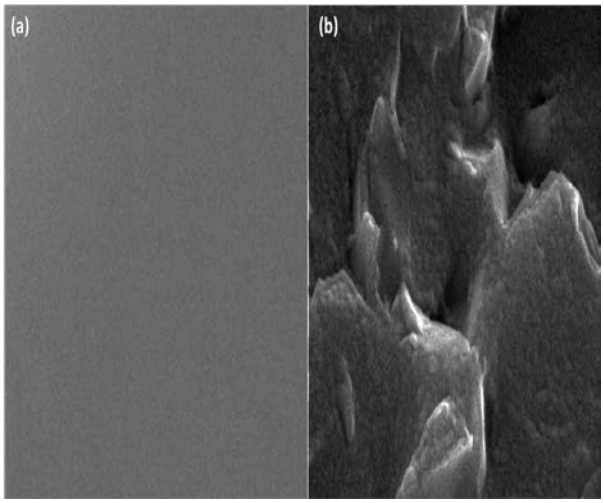

Figure 5: SEM micrograph of (a) virgin PTT, (b) PTT/C-93A clay nanocomposites

4.3.2 Transmission electron microscopy (TEM)

TEM micrograph of the mechanically optimized PTT/3% C-93A clay nanocomposites is presented in Fig. 6. The dark lines in Fig. 6 represent intersections of C-93A clay sheets while the grey part represents the PTT matrix. It can be evaluated that clay layers dispersed in the matrix is about 1–5 nm thick and 100–200 nm long and the spacing between layers exceeds 10 nm from Fig. 6. Therefore, the TEM result confirms the formation of exfoliated structure of the PTT/3% C-93A clay nanocomposites [12]. The orientation state of the clay sheets in the matrix is caused by the process of injection molding indicating the formation of intercalated nanocomposites [13].

Figure 6: TEM micrograph of PTT/C-93A clay nanocomposites

5. Conclusion

The work reported here describes the formation of PTT nanocomposites from PTT matrix and an organoclay (C-93A) through melt extrusion followed by micro-injection molding process. These formed PTT nanocomposites have been examined in order to elucidate the influences of the C-93A clay content, the better dispersion, and the better intercalation state confirmed by SEM and TEM analysis. The presence of C-93A organoclay within the PTT matrix was observed to have a reinforcing effect, as seen in the mechanical, thermal properties and morphologies of the PTT nanocomposites. In particular, the PTT/3% C-93A clay nanocomposites showed that the mechanical and thermal property was improved as well as heat deflection temperature. Furthermore, it was found that small amounts of organoclay were sufficient to improve the thermal stability and the mechanical properties of PTT matrix. In addition, when the clay content was increased from 3 to 5, the organoclay in the PTT matrix caused the ultimate mechanical and thermal properties to decrease due to debonding around the polymer–clay interfaces and void formation. The crystallisation and melting studies revealed that maximum transition peaks in the melting curves of the PTT/3% C-93A nanocomposites appeared virtually unchanged in the DSC thermograms. The crystallization phenomena start much earlier in PTT/3% C-93A clay nanocomposites. This is due to the fact that the clay particles act as a nucleating agent in the crystallization of PTT. Also it was found that the percentage crystallinity increases with increase in nanoclay content.

References

[1] S.W. Kim, W.H. Jo, M.S. Lee, M.B.Ko, and J.Y. Jho, Effects of shear on melt exfoliation of clay in preparation of nylon 6/organoclay nanocomposites, Polym. J. 34 (3), 2002, 103.

[2] I. Szleifer, and R. Yerushalmi-Rozen, Polymers and carbon nanotubes dimensionality, interactions and nanotechnology, Polymer. 46, 2005,7803.

[3] S. K. Nayak, S. Mohanty, Poly (trimethylene) terephthalate/m-LLDPE blend nanocomposites: Evaluation of mechanical, thermal and morphological behavior, Materials Science and Engineering A, 527, 2010, 574.

[4] W. Kunyan, C. Yanmo, and Z.Yu, Toughened poly(trimethylene terephthalate) by blending with a functionalized ethylene-propylene-diene copolymer, Polymer. 49,2008, 3301.

[5] Y. Kojima, A. Usuki, M. Kawasumi, A. Okada, T. Kurauchi, and O. Kamigaito, Novel preferred orientation in injection-molded nylon 6-clay hybrid, J. Polym. Sci. Part A Polym. Chem.31,1993, 983.

[6] K. Chen, X. Tang, S. Chen, G. Fu, Study on the macrokinetics of poly(trimethylene terephthalate) polycondensation reaction, J Appl Polym Sci, 92, 2004, 1765-1770,

[7] S. P. Dandurand, S. Pérez, J. F. Revol, and F. Brisse, The crystal structure of poly (trimethylene terephthalate) by X-ray and electron diffraction, Polymer, 20, 1979, 419-426.

[8] H. H. Chuah, Effect of process variables on bulk development of air-textured poly(trimethylene terephthalate) bulk continuous filament, J Appl Polym Sci, 92, 2004, 1011-1017,
[9] Y. Yang, H. Brown, and S. Li, Some sorption characteristics of poly (trimethylene terephthalate) with disperse dyes, J Appl Polym Sci, 86, 2002, 223-229,
[10] E. P. Giannelis, Polymer layered silicate nanocomposites. Adv Mater, 8(1), 1996, 29–35.
[11] G. Lagaly, Introduction: from clay mineral–polymer interactions to clay mineral–polymer nanocomposites. Appl Clay Sci. 15(1–2) 1999, 1–9.
[12] Z. Liu, K. Chen, and D. Yan, Nanocomposites of poly (trimethylene terephthalate) with various organoclays: morphology, mechanical and thermal properties. Polym Test, 23(3), 2004, 323–31.
[13] X. Hu, and A. J. Lesser. Effect of silicate filler on the crystal morphology of poly(trimethylene terephthalate)/clay nanocomposites. J Poly Sci B: Poly Phy, 41(19), 2003, 2275–89.
[14] K. L. Singfield, N. B. Djogbenou, Investigation of the multiple melting behavior of a PTT by DSC and polarized light optical microscopy, J Therm AnalCalorim, 86, 2006, 631-639.
[15] C. J. Ou, Nanocomposites of poly (trimethylene terephthalate) with organoclay. J App Poly Sci. 89(12), 2003, 3315–22.